Korean J. Chem. Eng., 39(1), 161-166 (2022)
DOI: 10.1007/s11814-021-0963-5

pISSN: 0256-1115
eISSN: 1975-7220

Catalytic removal of volatile organic compounds using black mass from spent batteries

Young-Kwon Park*, Wang Geun Shim, Sang-Chul Jung***, Ho-Young Jung****, and Sang Chai Kim*****,†**

*School of Environmental Engineering, University of Seoul, Seoul 02504, Korea
**Department of Chemical Engineering, Sunchon National University, Sunchon 57975, Korea
***Department of Environmental Engineering, Sunchon National University, Sunchon 57975, Korea
****Department of Environment and Energy Engineering, Chonnam National University, Gwangju 61186, Korea
*****Department of Environmental Education, Mokpo National University 61, Muan 58554, Korea
(*Received 2 August 2021 • Revised 27 September 2021 • Accepted 27 September 2021*)

Abstract−As battery usage increases every year, the number of spent batteries is also increasing, resulting in an important environmental issue. To examine the possibility of using the black mass (BM) obtained from spent batteries as a catalyst material for volatile organic compound (VOC) oxidation, the effect of the pretreating BM on its catalytic activity was investigated. Catalysts were prepared by pretreating the BM in three ways using water and sulfuric acid, and the catalytic performance of each catalyst was compared. The order of activity according to the pretreatment method was water and sulfuric acid hybrid pretreatment (WSBM)>sulfuric acid pretreatment (SBM)>water pretreatment (WBM)>raw (BM). The high adsorption energy site had a great influence on the activity of the catalyst. The number of acid sites and the easily movable lattice oxygen played an important role in the complete oxidation of benzene, toluene and o-xylene. At a gas hourly space velocity of 50,000 h^{-1}, benzene, toluene, and o-xylene were removed completely on the WSBM catalyst at 370 °C, 360 °C, and 350 °C, respectively.

Keywords: Volatile Organic Compounds, Catalytic Oxidation, Spent Batteries, Black Mass, Pretreatment

INTRODUCTION

Volatile organic compounds (VOCs) are persistent contaminants with high carcinogenic, mutagenic, and reproductive toxicity [1-4]. In addition, VOCs have been regarded as a major precursor of ground-level ozone and photochemical smog with air pollutants [5,6]. Therefore, they must be removed before being released into the atmosphere. Several technologies, such as thermal combustion, catalytic oxidation, adsorption, wet scrubbing and biofilter, have been adopted for VOC reduction [7,8]. Among them, catalytic oxidation is an efficient and stable technology for low-concentration VOC sources of less than 1% [9-11].

Manganese batteries have been used as power sources for many household goods, such as digital door locks, wall clocks, and toys, and thus, many are produced all over the world. As of 2002, more than 15 billion manganese batteries were produced in China [12, 13], and more than 4,000 tons of manganese/alkaline batteries were used annually in Korea in 2019 [14]. As a result of the increase in their use, large numbers of spent manganese batteries are generated annually, and their harmful components can contribute to environmental pollution. Therefore, recycling spent manganese batteries is essential for ecosystem protection and resource economics [12]. Much research has been conducted on recovering metals such as manganese and zinc in recycling spent batteries [15-18].

Spent manganese batteries contain manganese, zinc, and iron, which are active oxidation catalysts and are expected to be used as catalyst materials [19-21]. Tu et al. [22] reported on photocatalytic activity over zinc oxides prepared from Zn/Mn batteries, and Qu et al. [12] reported on photocatalytic degradation of organics in water using $Zn_xMn_{1-x}O$ prepared from Zn/Mn spent alkaline batteries. Gallegos et al. [23] applied Zn/Mn ferrite made from spent Zn/Mn batteries as an adsorbent to remove hazardous metals in water, and Deng et al. [24] used Zn/Mn ferrite as an auxiliary means of electrolytic operation to remove organic compounds. Also, Guo et al. [25] proposed VOC oxidation on multi-oxide catalysts fabricated on spent lithium-ion batteries using biohydrometallurgy, and Hoseini et al. [26] reported on VOC combustion over nano-manganese oxide catalysts made from spent batteries using chemical precipitation.

In this study, the black mass (BM) of spent batteries itself was intended to be used as a catalyst material for VOC oxidation. The effect of the treatment method on the catalytic activity was investigated because how BM is treated can affect its catalytic activity. Benzene, toluene, o-xylene (BTX) were selected as model substances for VOCs because they are causative agents of various diseases [27,28].

EXPERIMENT

1. Catalysts

BM, WBM, SBM, and WSBM catalysts were prepared for experiment according to preparation methods described in Supplementary Material (S1). The instrumental analyses conducted to investigate the catalyst properties, including ATR/IR, BET, SEM, XRD, NH_3-TPD, ICP/OES, and H_2-TPR, are also provided in Supplementary Material (S2).

†To whom correspondence should be addressed.
E-mail: gikim@mokpo.ac.kr

Table 1. Elements the catalysts according to treatment methods measured by ICP-OES

Element	BM (wt%)	WBM (wt%)	SBM (wt%)	WSBM (wt%)
Fe	5.76	8.57	8.43	9.06
Mn	30.60	42.50	36.00	38.70
Zn	34.80	32.00	10.40	11.10
Al	0.79	0.96	1.02	1.06
K	0.35	0.19	0.21	0.24
Na	0.09	0.03	0.03	0.04
Si	N.D.	N.D.	N.D.	N.D.

2. Catalytic Oxidation

BTX was completely oxidized in a reactor as described in earlier work [29]. In addition, Supplementary Material S3 provides the analytical methods and detailed experimental procedures.

RESULTS AND DISCUSSION

1. Catalyst Characterization

ICP/OES analysis was conducted to examine the components of the BM, WBM, SBM, and WSBM catalysts; Table 1 summarize the results. The constituents of all catalysts were Mn, Zn, Fe, Al, K, and Na. In catalysts excluding BM catalyst, Mn was the most abundant, followed by Zn, Fe, Al, K, and Na.

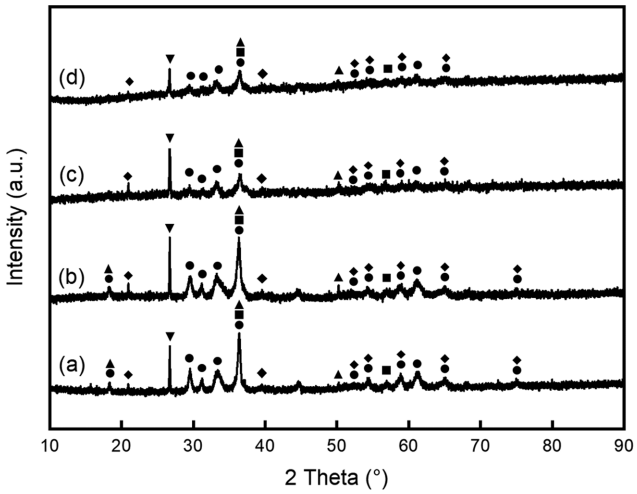

Fig. 1. XRD profiles (a) BM, (b) WBM, (c) SBM, and (d) WSBM catalysts.
● $ZnMn_2O_4$ ■ ZnO ▲ Mn_3O_4 ▼ C ◆ C_2K_2

XRD analysis was performed to investigate the crystalline structure of the prepared catalysts, and Fig. 1 displays the XRD patterns of four catalysts. The diffraction peaks for potassium carbide (C_2K_2), carbon (C), hausmannite (Mn_3O_4), zinc oxide (ZnO), and zinc dimanganate (III) ($ZnMn_2O_4$) phases appeared in the XRD profiles,

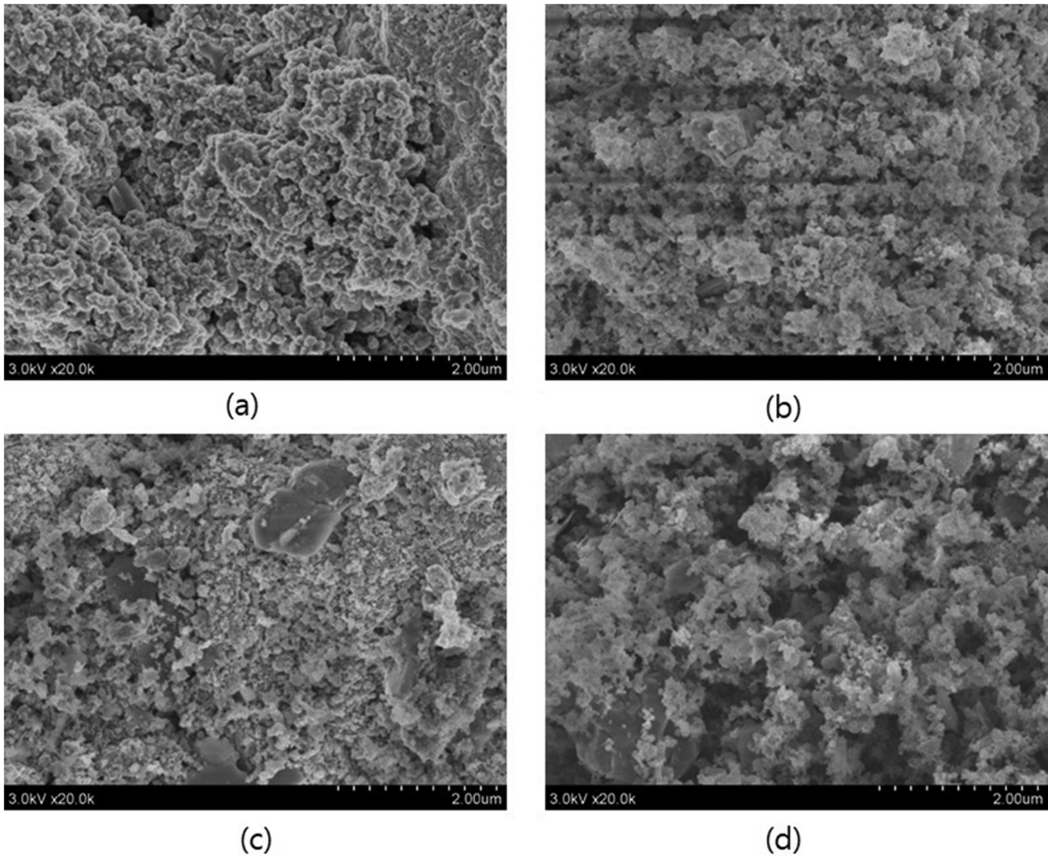

Fig. 2. SEM images of (a) BM, (b) WBM, (c) SBM, and (d) WSBM catalysts.

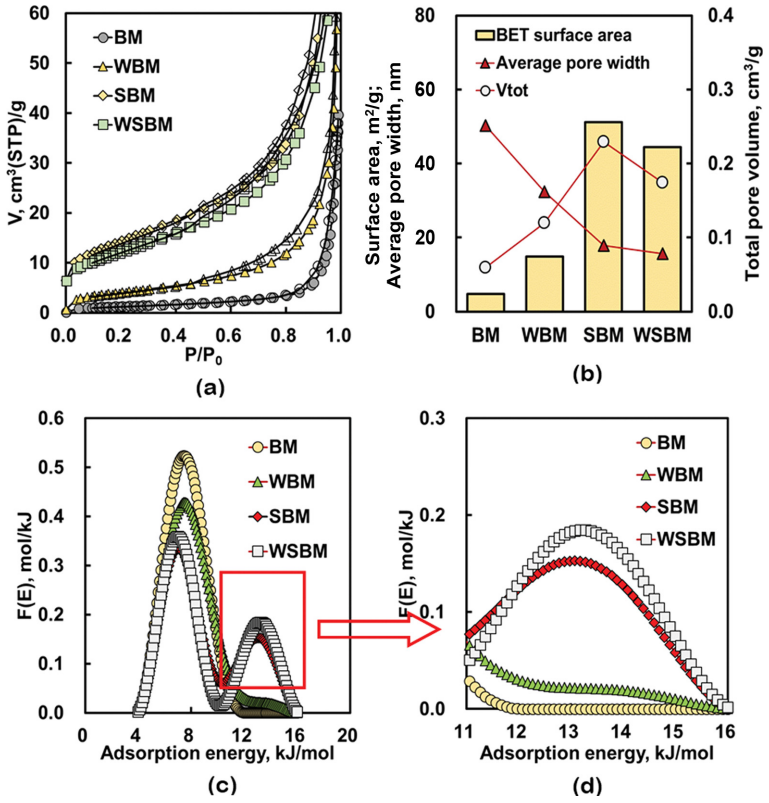

Fig. 3. Nitrogen adsorption (solid)-desorption (empty) isotherm curves of (a) BM, (b) WBM, (c) SBM, and (d) WSBM catalysts.

and the intensity of the crystalline phases decreased in the order of water treatment, sulfuric acid treatment, and water and sulfuric acid hybrid treatment.

The morphology of the BM, WBM, SBM, and WSBM catalysts was examined by SEM analysis. The SEM images of the catalysts are shown in Fig. 2. The image of the BM catalyst shows that small particles seem to be melted and agglomerated, while that of the WBM catalyst shows that the agglomerated small particles are released. Smaller particles formed in the SBM catalyst than in the WBM catalyst, and the WSBM catalyst appeared to have swollen particles.

Nitrogen adsorption analysis was used to comparatively investigate the relationship between the pretreatment conditions and the textural properties of samples, the results of which are summarized in Fig. 3 and Table 2. As shown in Fig. 3(a) and (b), the textural properties are greatly dependent on the pretreatment methods applied. Namely, the BET surface area and total pore volume of treated samples (WBM, SBM, WSBM) are much larger than those of the raw sample (BM), and the average pore widths of the treated samples are smaller than that of the raw sample, indicating that the applied pretreatment method plays a positive role in recovering the textural properties. By the IUPAC classification, the nitrogen isotherm shape of raw material follows type III, revealing the existence of weak interactions between adsorbate and adsorbent, while the pretreated samples show type IV with the type H3 hysteresis loops indicating the existence of slit-shaped pores (Fig. 3(a)) [30]. In addition, the BET surface area and the total pore volume are in the following order: sulfuric acid treatment (SBM)>water and sulfuric acid hybrid treatment (WSBM)>water treatment (WBM)>raw (BM). On the whole, the pretreated samples exhibited narrower average pores than did the raw sample, but the average pore width of the WSBM sample is slightly smaller than that of the SBM sample. This result clearly indicates that the sulfuric acid and hybrid treatment methods (water and sulfuric acid) are the most suitable for recovering the textural properties of raw BM sample.

Table 2. Textural properties of SB (400) according to treatment methods

Catalyst	BM	WBM	SBM	WSBM
BET surface area ($m^2\ g^{-1}$)	4.72	14.82	51.21	44.40
Total pore volume ($cm^3\ g^{-1}$)	0.06	0.12	0.22	0.17
Average pore width (nm)	50.24	32.37	17.89	15.73

Nitrogen adsorption energy distribution function was used to further comparatively examine the surface energetic heterogeneity of the samples before and after pretreatment. As compared in Fig. 3(c) and (d), the AED shape and patterns are greatly dependent on the pretreatment methods applied. Namely, the raw sample shows unimodal distribution curve, but the sulfuric acid and hybrid treated samples show bimodal curves. In addition, the peak intensity in the high adsorption energy region increased significantly after the sulfuric acid and hybrid treatments, which could be closely related to the partial removal of blocked residues present in the raw sample.

The surfaces of the catalysts were investigated using ATR/FTIR,

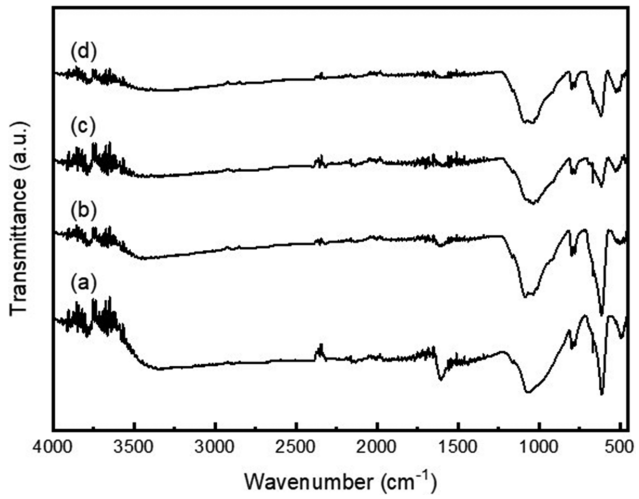

Fig. 4. ATR/FTIR spectra of (a) BM, (b) WBM, (c) SBM, and (d) WSBM catalysts.

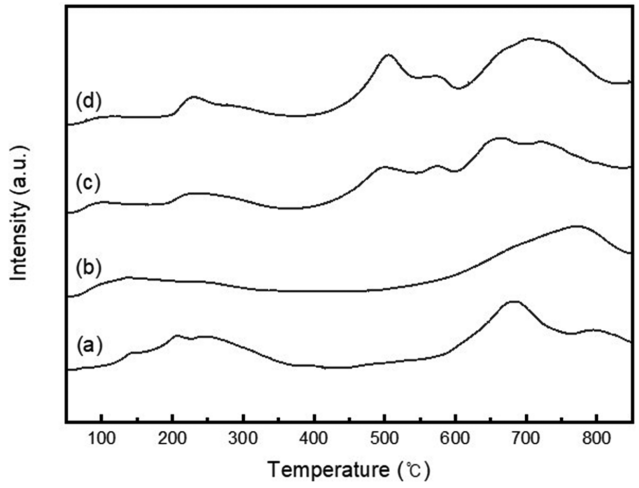

Fig. 5. TPD patterns of (a) BM, (b) WBM, (c) SBM, and (d) WSBM catalysts.

and Fig. 4 presents the ATR/FTIR spectra of the BM, WBM, SBM, and WSBM catalysts. In the BM spectrum, the broad peak of 3,403 cm^{-1} and the peak of 1,606 cm^{-1} are attributed to the stretching vibration of the OH group and C=C, respectively [31,32]. However, both peaks gradually decreased in the order of WBM, SBM, and WSBM catalyst. This reduction seems to be attributable to the partial removal of blocked residues present in the raw sample, as shown in Fig. 4(c) and (d).

The NH_3-TPD experiment was performed to find the effect of

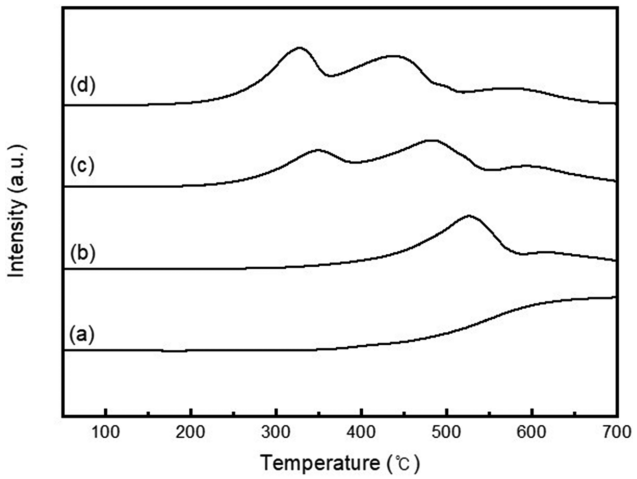

Fig. 6. TPR patterns of (a) BM, (b) WBM, (c) SBM, and (d) WSBM catalysts.

catalysts acid on the catalytic activity. Fig. 5 shows the NH_3-TPD patterns of the BM, WBM, SBM, and WSBM catalysts and Table 3 lists the amount of their ammonia desorption. The number of WSBM acid sites (6.07 mmol/g) was the largest, followed by SBM (5.30 mmol/g), WBM (4.28 mmol/g), and BM (4.01 mmol/g) in order.

The redox property of a catalyst often plays an important role in catalytic oxidation. Therefore, the redox property of the BM, WBM, SBM, and WSBM was studied by H_2-TPR experiments. Their TPR profiles are shown in Fig. 6. In addition, Table 3 lists the temperatures of TPR peak (TTP). One broad reduction peak in the range of 400 °C to 700 °C was observed in the BM. For the WBM, one distinct reduction peak and another broad reduction peak appeared at 527 and 620 °C, respectively. Three reduction peaks were observed in SBM and WSBM, 350, 482, and 592 °C and 327, 437, and 571 °C, respectively. That is, the WSBM TTP was the lowest, followed by SBM<WBM<BM.

2. Oxidation Reaction

To examine the catalytic activity of the BM, WBM, SBM, and WSBM catalysts, the BTX was completely oxidized according to the reaction temperature. Fig. 7 shows the BTX conversion curves for the BM, WBM, SBM, WSBM catalysts. Tables 4, 5, and 6 present the temperature for 50% conversion (T_{50}) and the temperature for 90% conversion (T_{90}) for BTX. For all reactants (BTX), the T_{50} and T_{90} for all catalysts in the order of low temperature, that is, in order of catalytic activity, was WSBM<SBM<WBM<BM. In addition, in the case of BM, benzene conversion did not reach 50% even at 500 °C, and toluene conversion did not reach 90% at 500 °C.

Repeated experiments were conducted to confirm the stability

Table 3. Amount of ammonia desorption and temperatures of TPR peak of the catalysts

Catalyst	BM	WBM	SBM	WSBM
Total ammonia desorption (mmol/g)	4.01	4.28	5.30	6.07
Temperature of TPR peak (°C)	550[a]	527[a], 620[b]	350[a], 482[b], 592[c]	327[a], 437[b], 571[c]

[a]1st peak, [b]2nd peak, [c]3rd peak

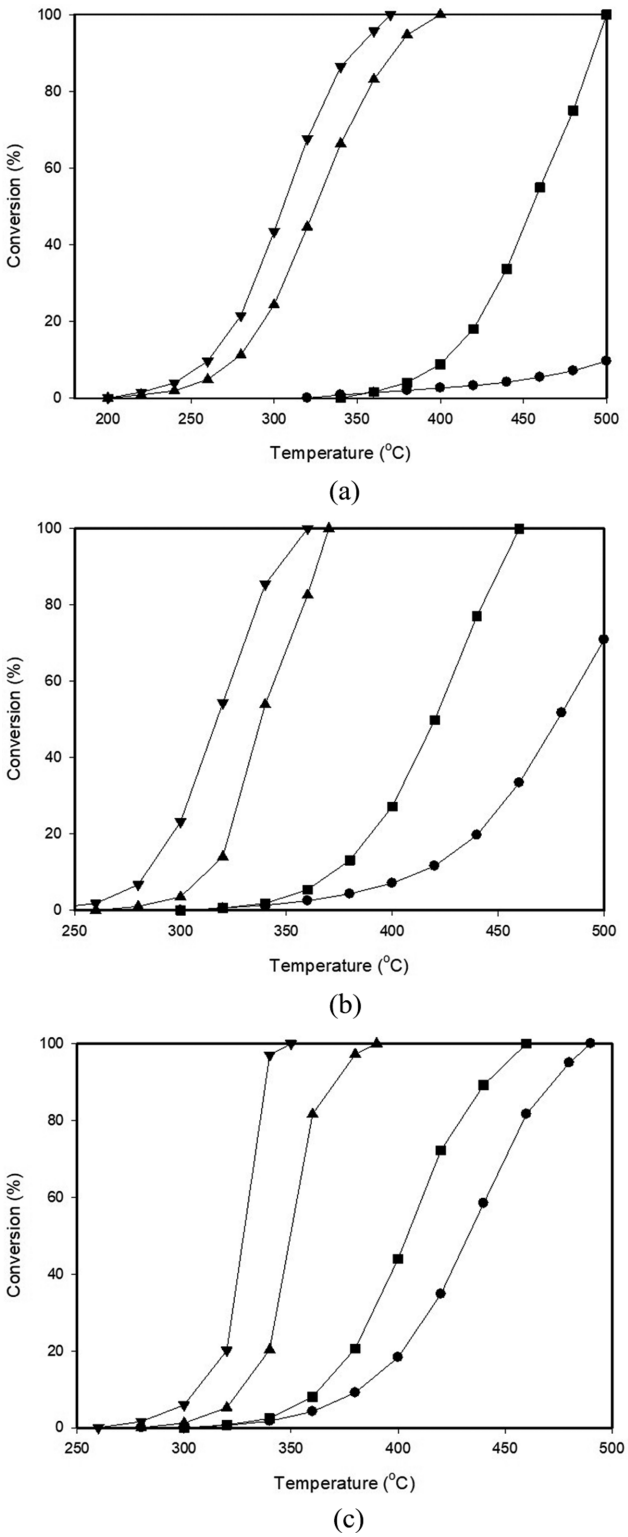

Fig. 7. Benzene (a), toluene (b), and o-xylene (c) conversions according to reaction temperature (Reaction conditions: reactant concentration=1,000 ppm, GHSV=50,000 h^{-1}).
● BM ■ WBM ▲ SBM ▼ WSBM

of the most active catalyst, the WSBM. Fig. 8 displays the effects of three consecutive catalytic tests on the toluene conversion curves;

Table 4. T_{50} and T_{90} of benzene conversion according to the catalysts

Catalyst	BM	WBM	SBM	WSBM
T_{50} (°C)	-	455	324	305
T_{90} (°C)	-	492	372	348

Table 5. T_{50} and T_{90} of toluene conversion according to the catalysts

Catalyst	BM	WBM	SBM	WSBM
T_{50} (°C)	478	420	338	317
T_{90} (°C)	-	451	364	346

Table 6. T_{50} and T_{90} of o-xylene conversion according to the catalysts

Catalyst	BM	WBM	SBM	WSBM
T_{50} (°C)	432	404	349	328
T_{90} (°C)	473	441	370	338

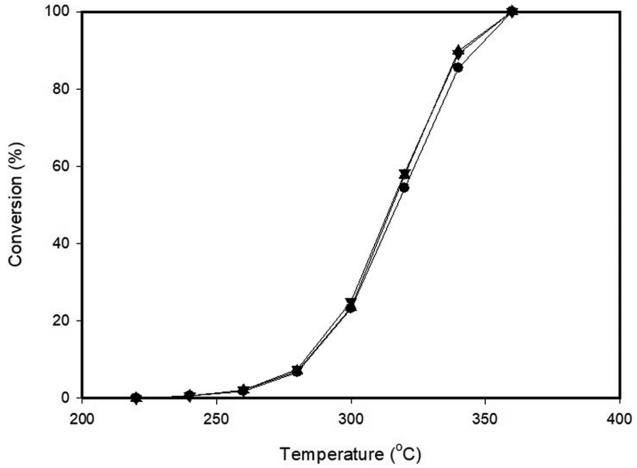

Fig. 8. Toluene conversions according to reaction temperature over WSBM catalyst (Reaction conditions: reactant concentration=1,000 ppm, GHSV=50,000 h^{-1}).
● 1st run ▲ 2nd run ▼ 3rd run

after each catalytic run, the catalytic reactor was purged in N_2 flow at 150 °C for 1 h to clean the catalyst surface. As shown in Fig. 8, the first, second and third catalytic runs gave almost the same results; therefore, the WSBM was considered to be quite stable.

The order of catalytic activity was WSBM>SBM>WBM>BM, which coincides with the order of the number of high adsorption energy sites from the result of the nitrogen adsorption energy distribution function (Fig. 3(d)). In brief, the more high adsorption energy sites, the greater the catalytic activity [33]. The NH_3-TPD results indicated that the order of the number of acid sites was WSBM (6.07 mmol/g)>SBM (5.30 mmol/g)>WBM (4.28 mmol/g)> BM (4.01 mmol/g), and these values were in good agreement with the catalytic activity. Therefore, the number of acid sites played an important role in the complete oxidation of BTX. In addition, TPR results showed that the TTP of the WSBM was the lowest, followed by SBM, WBM, and BM in order. This result indicates that the lower the TTP, the greater the catalytic activity. Several research teams

reported that the easier the lattice oxygen of the catalyst moves, the more favorable the conditions for the complete oxidation of hydrocarbons [20,34,35]. As a result, the easily movable lattice oxygen significantly contributed to the complete oxidation of VOCs.

CONCLUSIONS

The complete oxidation of BTX was carried out to study the effect of the BM pretreatment method on its catalytic activity. The order of activity according to the pretreatment method was water and sulfuric acid hybrid (WSBM)>sulfuric acid (SBM)>water (WBM)>raw (BM), which coincided with the order of peak intensity in the high adsorption energy region from the result of the nitrogen adsorption energy distribution function. The greater the strength of adsorption sites, the better the activity of the catalyst, and the number of acid sites by catalyst was WSBM>SBM>WBM> BM; this order was in good agreement with that of the catalytic activity. Therefore, the number of acid sites had an important effect on the complete oxidation of BTX. The TTP of the WSBM was the lowest, followed by SBM, WBM, and BM in order, indicating that the lower the TTP, the greater the catalytic activity. The easily movable lattice oxygen significantly contributed to the complete oxidation of VOCs. Thus, the strength of adsorption sites, the number of acid sites, and readily movable lattice oxygen played important roles in complete VOC oxidation. At a gas hourly space velocity of 50,000 h^{-1}, benzene, toluene, and o-xylene were oxidized completely on the WSBM catalyst at 370 °C, 360 °C, and 350 °C, respectively.

ACKNOWLEDGEMENTS

This research was supported by the Basic Science Research Program the National Research Foundation of Korea (NRF) funded by the Ministry of Science and ICT (2019R1F1A1050281).

SUPPORTING INFORMATION

Additional information as noted in the text. This information is available via the Internet at http://www.springer.com/chemistry/journal/11814.

REFERENCES

1. D. Belpomme, P. Irigaray, L. Hardell, R. Clapp, L. Montagnier, S. Epstein and A. J. Sasco, *Environ. Res.*, **105**, 414 (2007).
2. D. Sarigiannis, S. Karakitsios, A. Gotti and I. Liakos, *Environ. Int.*, **37**, 743 (2011).
3. H. Guo, S. C. Lee, L. Y. Chan and W. M. Li, *Environ. Res.*, **94**, 57 (2004).
4. Q. Wang, K. L. Yeung and M. A. Bañaresd, *Catal. Today*, **356**, 141 (2020).
5. Z. Li, D. P. Yang, Y. Chen, Z. Du, Y. Guo, J. Huang and Q. Li, *Mol. Catal.*, **483**, 110766 (2020).
6. Y. Tan, S. Han, Y. Chen, Z. Zhang, H. Li, W. Li, Q. Yuan, X. Li, T. Wang and S. C. Lee, *Sci. Total Environ.*, **777**, 146241 (2021).
7. Z. Zhang, Z. Jiang and W. Shangguan, *Catal. Today*, **264**, 270 (2016).
8. J. E. Lee, Y. S. Ok, D. C. W. Tsang, J. H. Song, S. C. Jung and Y. K. Park, *Sci. Total Environ.*, **719**, 137405 (2020).
9. M. S. Kamal, S. A. Razzak and M. M. Hossain, *Atmos. Environ.*, **140**, 117 (2016).
10. N. Abbas, M. Hussain, N. Russo and G. Saracco, *Chem. Eng. J.*, **175**, 330 (2011).
11. Z. Jamalzadeh, M. Haghighi and N. Asgari, *Front. Environ. Sci. Eng.*, **7**, 365 (2013).
12. J. Qu, Y. Feng, Q. Zhang, Q. Cong, C. Q. Luo and X. Yuan, *J. Alloys Compd.*, **622**, 703 (2015).
13. J. M. Nan, D. M. Han, M. Cui, M. J. Yang and L. M. Pan, *J. Hazard. Mater.*, **133**, 257 (2006).
14. KRBA, 2019 (Korea Battery Recycling Association) Report.
15. Z. Yao, Z. Huang, Q. Song, Y. Tang, R. Qiu and J. Ruan, *J. Cleaner. Prod.*, **278**, 123867 (2021).
16. X. Hu, A. Robles, T. Vikstrom, P. Vaananen, M. Zackrisson and G. Ye, *J. Hazard. Mater.*, **411**, 124928 (2021).
17. S. A. Charef, A. M. Affoune, A. Caballero, M. Cruz-Yusta and J. Morales, *Waste. Manage.*, **68**, 518 (2017).
18. B. Ebin, M. Petranikova, B. M. Steenari and C. Ekberg, *Waste. Manage.*, **68**, 508 (2017).
19. F. G. Durán, B. P. Barbero, L. E. Cadús, C. Rojas, M. A. Centeno and J. A. Odriozola, *Appl. Catal. B: Environ.*, **92**, 194 (2009).
20. S. C. Kim and W. G. Shim, *Appl. Catal. B: Environ.*, **98**, 180 (2010).
21. H. Wu, L. Wang, J. Zhang, Z. Shen and J. Zhao, *Catal. Commun.*, **12**(10), 859 (2011).
22. Y. J. Tu, C. F. You and C. K. Chang, *J. Hazard. Mater.*, **258-259**, 102 (2013).
23. M. V. Gallegos, F. Aparicio, M. A. Peluso, L. C. Damonte and J. E. Sambeth, *Mater. Res. Bull.*, **103**, 158 (2018).
24. B. Deng, Y. T. Li, W. H. Tan, Z. X. Wang, Z. W. Yu, S. Y. Xing, H. Lin and H. Zhang, *Chemosphere*, **204**, 178 (2018).
25. M. Guo, K. Li, L. Liu, H. Zhang, W. Guo, X. Hu, X. Meng, J. Jia and T. Sun, *J. Hazar. Mater.*, **380**, 120905 (2019).
26. S. Hoseini, N. Rahemi, S. Allahyari and M. Tashihi, *J. Cleaner Prod.*, **232**, 1134 (2019).
27. D. Belpomme, P. Irigaray, L. Hardell, R. Clapp, L. Montagnier, S. Epstein and A. J. Sasco, *Environ. Res.*, **105**, 414 (2007).
28. J. Huff, P. Chan and R. Melnick, *Regul. Toxicol. Pharmacol.*, **58**, 167 (2010).
29. S. C. Kim, S. W. Nahm and Y. K. Park, *J. Hazard. Mater.*, **300**, 104 (2015).
30. F. Rouquerol, J. Rouguerol and K. Sing, *Adsorption by powders and porous solids. Principles, methodology and applications*, Academic Press, London (1999).
31. C. H. Rochester and S. A. Topham, *J. Chem. Soc. Faraday Trans.*, **75**, 1073 (1979).
32. C. A. Hepburn, P. Vale, A. S. Brown, N. J. Simms and E. J. McAdam, *Talanta*, **141**, 128 (2015).
33. W. G. Shim and S. C. Kim, *Appl. Sur. Sci.*, **256**, 5566 (2010).
34. J. Trawczyński, B. Bielak and W. Miśta, *Appl. Catal. B Environ.*, **55**, 277 (2005).
35. S. Scirè, S. Minicò, C. Crisafulli and S. Galvagno, *Catal. Commun.*, **2**(6-7), 229 (2001).

Supporting Information

Catalytic removal of volatile organic compounds using black mass from spent batteries

Young-Kwon Park*, Wang Geun Shim, Sang-Chul Jung***, Ho-Young Jung****, and Sang Chai Kim*****,†**

*School of Environmental Engineering, University of Seoul, Seoul 02504, Korea
**Department of Chemical Engineering, Sunchon National University, Sunchon 57975, Korea
***Department of Environmental Engineering, Sunchon National University, Sunchon 57975, Korea
****Department of Environment and Energy Engineering, Chonnam National University, Gwangju 61186, Korea
*****Department of Environmental Education, Mokpo National University 61, Muan 58554, Korea
(*Received 2 August 2021 • Revised 27 September 2021 • Accepted 27 September 2021*)

1. Text S1

(1) BM catalyst: The black mass was then dried in an oven at 80 °C for 24 h. The dried samples were calcined for 4 h in a furnace at 400 °C.

(2) WBM catalyst: The BM (3 g) was placed in a 50 mL deionized water flask, and then the resulting mixture was stirred at 150 rpm for 5 h at room temperature in a shaker (KMC-8480SF, Vision Scientific Co., Korea) The stirred mixture was filtered and washed three times using deionized water. The sample was then dried in an oven at 80 °C for 24 h. The dried samples were calcined for 4 h in a furnace at 400 °C.

(3) SBM catalyst: the BM (3.0 g) was added into a flask containing 200 mL of 0.1 N sulfuric acid solution, after which the mixture was stirred at 150 rpm at 30 °C for 5 h in a shaker. The sample treated with acid was further washed using deionized water until the pH of the samples reached about 7. The sample was then dried in an oven at 80 °C for 24 h. The dried samples were calcined for 4 h in a furnace at 400 °C.

(4) WSBM catalyst: The WBM sample without drying and calcination (3.0 g) was added into a flask containing 200 mL of 0.1 N sulfuric acid solution, and then the mixture was stirred at 150 rpm at 30 °C for 5 h in a shaker. The sample treated with acid was further washed using deionized water until the pH of the samples reached about 7. The sample was then dried in an oven at 80 °C for 24 h. The dried samples were calcined for 4 h in a furnace at 400 °C.

2. Text S2

Brunauer-Emmett-Teller (BET) measurements were performed using a Belsorp Mini II 2020 to determine the surface areas of the catalysts (N_2 adsorption at 25 °C). Before sorption analysis, all catalysts were degassed in a vacuum (5×10^{-3} mmHg) at 150 °C for 6 h. The elemental compositions of the catalysts were analyzed by inductively coupled plasma optical emission spectroscopy (ICP/OES) using a Perkin Elmer Optima 8300. The samples were prepared for analysis using the microwave-assisted acid (aqua regia) digestion method. X-ray diffraction (XRD) was used to study the crystalline structures of the catalysts using a Phillips PW3123 diffractometer with Cu/Kα radiation of 0.154 nm. The catalysts were examined in the 2θ range of 20-90° at a scanning speed of 70° h^{-1}. Scanning electron microscopy (SEM) measurements were conducted using a Hitachi S-4800 SEM to investigate the morphologies of the catalysts. Attenuated total reflection/Fourier transform infrared spectrophotometry (ATR/FTIR) measurements were performed using a Bio-Rad FTS 60A to study the catalyst surface. An ATR/FTIR spectrum was obtained in the range of 400 to 4,000 cm^{-1} with a spectral resolution of 4 cm^{-1}. The redox of the catalysts was examined by hydrogen temperature programmed reduction (H_2-TPR) using a BEL-CAT setup. Prior to analysis, 0.4 g of the catalyst was pre-treated with 30 cm^3 min^{-1} of Ar gas at 200 °C for 2 h. The temperature of the catalyst was then lowered to 50 °C. The catalyst sample was passed through the gas mixture (5% H_2 and 95% Ar) at a rate of 30 mL min^{-1} while the temperature was increased to 1,000 °C at a rate of 10 °C min^{-1}. Acid sits of the catalysts were measured by ammonia temperature programmed desorption (NH_3-TPD) using a BEL-CAT setup. 0.4 g of the catalyst was pre-treated with 30 cm^3 min^{-1} of He gas at 200 °C for 2 h. The temperature of the catalyst was then lowered to 50 °C. The catalyst sample was passed through a gas mixture (5% NH_3 and 95% He) for 1 hour at a rate of 30 mL min^{-1}, purged with helium gas for 30 minutes, and finally increasing to 900 °C at a rate of 10 °C min^{-1}.

3. Text S3

60 mg of catalyst sample was supported with quartz wool and filled in the middle of the reactor. Benzene, toluene, and o-xylene acquired from Fisher were used without any further treatment. Air was bubbled through a saturator filled with benzene, toluene, and o-xylene. Mass flow controllers (UNIT Instrument, UFC-8100) were used to accurately and stably control the flow rates of gas. Each reactant was mixed with another air stream at controlled temperature at the saturator while the reactant flows were converted at 50,000 h^{-1} of gas hourly space velocity (GHSV). To prevent the condensation and adsorption of the product or reactant inside the tubes, all lines were fully heated to 120 °C and the experimental data were collected.

Concentrations of outlet and inlet gas streams were examined with a gas chromatograph (GC-14A model, Shimazu) connected with a thermal conductivity detector (TCD). The chromatographic columns used consist of a parapak Q (50-80 mesh, 3 mm ø×3 m) for CO_2 separation, while o-xylene analysis used a 5% bentone-34 and 5% DNP/shimalite (60-80 mesh, 3 mm ø×3 m). GC/MS (Shimadzu, QP5050) with a flame ionization detector (FID) was also

used to analyze the final products and by-products qualitatively and its chromatographic column was DB 624 (0.25 mm ø×60 m). The experimental procedure in the present work produced only H_2O and CO_2. The conversion was calculated from the carbon balance according to the consumption of reactant and the production of carbon dioxide.